

Received August 6, 2020, accepted August 26, 2020, date of publication September 3, 2020, date of current version September 18, 2020.

Digital Object Identifier 10.1109/ACCESS.2020.3021051

Tractor Assistant Driving Control Method Based on EEG Combined With RNN-TL Deep Learning Algorithm

WEI LU^{1,2}, (Member, IEEE), YUNING WEI^{1,2}, JINXIA YUAN³,
YIMING DENG⁴, (Senior Member, IEEE), AND
AIGUO SONG⁵, (Senior Member, IEEE)

¹College of Engineering, Nanjing Agricultural University, Nanjing 210031, China

²Jiangsu Key Laboratory of Intelligent Agricultural Equipment, Nanjing Agricultural University, Nanjing 210031, China

³School of Education Science, Nanjing Normal University, Nanjing 210097, China

⁴College of Engineering, Michigan State University, East Lansing, MI 48824, USA

⁵School of Instrument Science and Engineering, Southeast University, Nanjing 210096, China

Corresponding author: Wei Lu (njurobot@njau.edu.cn)

This work was supported in part by the National Natural Science Foundation of China under Grant 31960487, in part by the Natural Science Foundation of Jiangsu Province under Grant BK20181315, in part by the Three New Agricultural Project in Jiangsu Province under Grant SZ120170036, and in part by the Asia Hub NAU-MSU Joint Project under Grant 2017-AH-11.

ABSTRACT Nowadays, fieldwork is often accompanied by tight schedules, which tends to strain the shoulder muscles due to high-intensity work. Moreover, it is difficult and stressful for the disabled to drive agricultural machinery. Besides, current artificial intelligence technology could not fully realize tractor autonomous driving because of a high uncertain filed environment and short interruptions of satellite navigation signal shaded by trees. To reduce manual operations, a tractor assistant driving control method was proposed based on the human-machine interface utilizing the electroencephalographic (EEG) signal. First, the EEG signals of the tractor drivers were collected by a low-cost brain-computer interface (BCI), followed by denoising using a wavelet packet. Then the spectral features of EEG signals were calculated and extracted as the input of Recurrent Neural Network (RNN). Finally, the EEG-aided RNN driving model was trained for tractor driving robot control such as straight going, brake, left turn, and right turn operations, which control accuracy was 94.5% and time cost was 0.61 ms. Also, 8 electrodes were selected by the PCA algorithm for the design of a portable EEG controller. And the control accuracy reached 93.1% with the time cost of 0.48 ms. To solve the incomplete driving data set in the actual world because some driving manners may cause dangerous or even death, RNN-TL algorithm was employed by creating the complete driving data in the virtual environment followed by transferring the driving control experience to the actual world with small actual driving data set in the field, which control accuracy was 93.5% and time consumption was 0.48 ms. The experimental results showed the feasibility of the proposed tractor driving control method based on EEG signal combined with RNN-TL deep learning algorithm which can work with the displacement error less than 6.7 mm when the tractor speed is less than 50 km/h.

INDEX TERMS Electroencephalographic (EEG), brain-computer interface (BCI), recurrent neural network (RNN), assistant driving, driving robot.

I. INTRODUCTION

Agricultural machinery is popularly used in most field operations such as tillage, harvesting, weeding, and land preparation for improving agricultural efficiency. Whereas the shoulder muscles of drivers are vulnerable due to the

The associate editor coordinating the review of this manuscript and approving it for publication was Jinpeng Yu¹.

high-intensity repetitive operation of quick steering during the busy farming season [1]. Furthermore, it is extremely easy to cause fatigue driving and lead to traffic accidents every year. Moreover, unexpected risk is increased because of hazard working environment, extreme weather conditions and high-intensity work due to limited crop harvesting time which will lead to fatigue of drivers. Besides, the traditional agricultural machinery cannot satisfy the operation of

the disabled drivers whose proportion is about one fifth in America.

The intelligent navigation method such as the Global Navigation Satellite System (GNSS) [2], [3] was introduced to tractor autonomous driving in the field but will fail intermittently because of the satellite signal blocked by the trees occasionally.

Machine vision navigation technology [4] as an auxiliary navigation method was developed for covering the shortage of GNSS but can not work all the time because of the tremendous complexity and uncertainty in the farmland.

Since electroencephalogram (EEG) signal is the direct embodiment of human brain consciousness, the auxiliary driving method based on the EEG signal can reduce the driver's workload, improve work precision, avoid disastrous consequences caused by driver fatigue operation, and provide a feasible solution for the disabilities to drive agricultural machinery as well.

The brain-computer interface (BCI) technology provides a new solution for tractor assistant driving because the BCI technology has been widely used in fatigue detection [5], [6], emotion recognition [7], [8], mental task classification [9]–[15], robot control and the disabled assistive help [16], [17], etc. in recent years. Nowadays, BCI technology has been applied in the assistant driving of airplanes, automobiles, and other vehicles successfully to achieve steering, U-turn control, tracking control [18]–[21], etc.

Nowadays, EEG was popularly used in actuator control in different fields. Alyasseri, Z. A. A. proposed Flower Pollination Algorithm (FPA) combined with wavelet transformation to denoise EEG signals, extract features and classify effectively, which accuracy reached 87.69% [9]–[13]. Moreover, the improved MOFPA-WT algorithm can remove EOG artifacts and the classification precision reached 97.5% [14], [15]. Bartosz Binias utilized EPOC+ electroencephalograph combined with Common Spatial Pattern (CSP) algorithm, band-pass filtering method, and neural network classifiers for monitoring and enhancing the performance of aircraft pilots [19]. In addition, EPOC+ was also used by J. Gomez-Gil in tractor steering control with a deviation of less than 7 cm from the standard track which shows the feasibility of tractor driving based on EEG [21].

In this article, we proposed a tractor assistant driving technology based on the EEG signal and tested on the second generation of tractor driving robot platform developed by our lab [22]–[24]. The rest of the paper was organized as follows: First, the experimental platform and method were introduced. Then the signal processing, feature extraction, and control method were mentioned. Finally, the experiments were carried out and the results were discussed and concluded.

II. MATERIALS AND METHODS

A. MATERIALS

1) SUBJECT

Factors such as age, physical condition, and the fatigue level of the subjects directly influence the experimental results.

Fifteen volunteers including 10 males and 5 females were selected as subjects in the experiments. All subjects were all healthy, sighted without any brain disease whose ages ranged from 20 to 25 years old. Also, the experiments were carried out at different times of the day for improving the robustness of the motion intention recognition model.

2) EXPERIMENTAL SETUP

a: EEG ACQUISITION DEVICE

The EEG signals were recorded by the Emotiv-EPOC+ system (Fig.1a), which has been applied in the tractor tracking control by the University of Valladolid in Spain [21]. The device has 14 electrodes to collect different areas EEG signals on the head and the electrodes were placed according to the 10/20 electrode placement system (Fig.1b).

EEG signals were collected and processed on an industrial computer, configured with an Intel Core i5 processor, 8G memory, Windows 10 operating system, and a programming environment of Matlab R2019a.

b: DRIVING ROBOT

Figure 2 shows the second-generation human-machine cooperative tractor driving robot developed by our lab. The structure mainly includes a steering manipulator, a shift manipulator, a rotary tiller lifting manipulator, a break-leg, a clutch-leg, and a throttle-leg in Figure 3. The steering manipulator can control the tractor's steering wheel smoothly. The shift manipulator can change the gears. The clutch-leg and break-leg are responsible for the clutch and brake operations of the tractor. The throttle-leg is used for the gas adjustment of the tractor. The driving robot adopts hybrid control modes, i.e., the break-leg, clutch-leg, and rotary tiller lifting manipulator are hydraulically driven and other manipulations are electrically controlled.

In order to control the tractor more intelligently and achieve safe and efficient operation simultaneously, the tractor driving robot was controlled on the hybrid switching mode, i.e., GNSS navigation control is preferred for the tractor and EEG control mode will be used when the GNSS navigation signal is lost or any other emergency cases occur. Hence, it can relieve drivers' work intensity and provide a feasible way for the disabled driving tractors in the complicated agricultural environment as well. This article focuses on studying the tractor control method by EEG signal.

B. EEG SIGNAL ACQUIRING METHOD

For improving the recognition precision and model robustness, the training set was built based on the experiments carried out according to the method below. Firstly, the experiments were executed at different times of a day such as morning, noon, and afternoon for acquiring EEG data of the subjects in different states of mind and fatigue. Second, the subjects were trained 3 minutes before the experiments. Finally, the experiments were conducted according to the steps below.



FIGURE 1. Emotiv EPOC+ and electrode setting. a) the Emotiv-EPOC+ system. b) 10/20 electrode placement system.



FIGURE 2. The second-generation human-machine cooperative tractor driving robot was developed by our lab which structure is showed in Figure 3. The subjects sat in the tractor and controlled the tractor-driving robot based on EEG signal for straight going, brake, left turn, and right turn.



FIGURE 3. The overall arrangement of the driving robot. Among them, 1 is the steering manipulator, 2 is the hydraulic drive, 3 is the pedal control mechanical leg, including a break-leg, a clutch-leg, and a throttle-leg, 4 is the shift manipulator.

- 1) The subjects were led to concentrate on the experiment by a cross shown on the center of the screen for 3 s.
- 2) To acquire the EEG signals of the subjects while they creating imagery movement according to the displaying animations in the screen randomly.

3) Previous EEG signal cleaning step by 5 s relaxation was used to attenuate the brain activity that had been generated by the previous stimulus [8], [25].

It should be noted that step 1 and step 3 mentioned above were not used during the test experiments. The subject made a decision to go straight, left turn, right turn, or brake according to the condition of the lane displayed in the screen and at the same time, the EEG signal of the subject was collected and processed to control the virtual car in the game. The same EEG signal acquiring method was adopted during actual tractor driving control using a tractor driving robot.



FIGURE 4. Imagine according to the animation content.

C. CONTROL METHODS BASED ON EEG

1) TRACTOR DRIVING MODEL BASED ON EEG IN THE VIRTUAL ENVIRONMENT

The control model based on EEG for tractor driving was carried out in the virtual environment for avoiding fatal dangerous and financial loss during physical experiments in the actual tractor test field.

The specific experimental steps are as follows shown in Figure 6. Firstly, the EEG signals of the subjects were collected by using the Emotiv-EPOC+ system followed by denoising using a Butterworth low-pass filter. Then the features of the power spectrum signal of driving actions were extracted by the wavelet packet. Finally, the obtained features

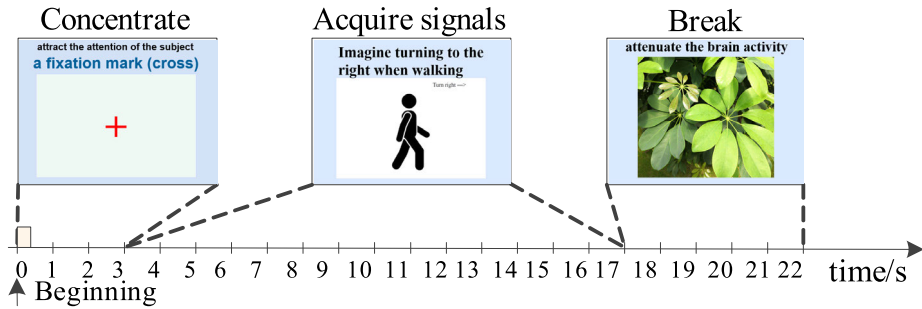


FIGURE 5. Time paradigm of EEG acquisition for a sports imagination.

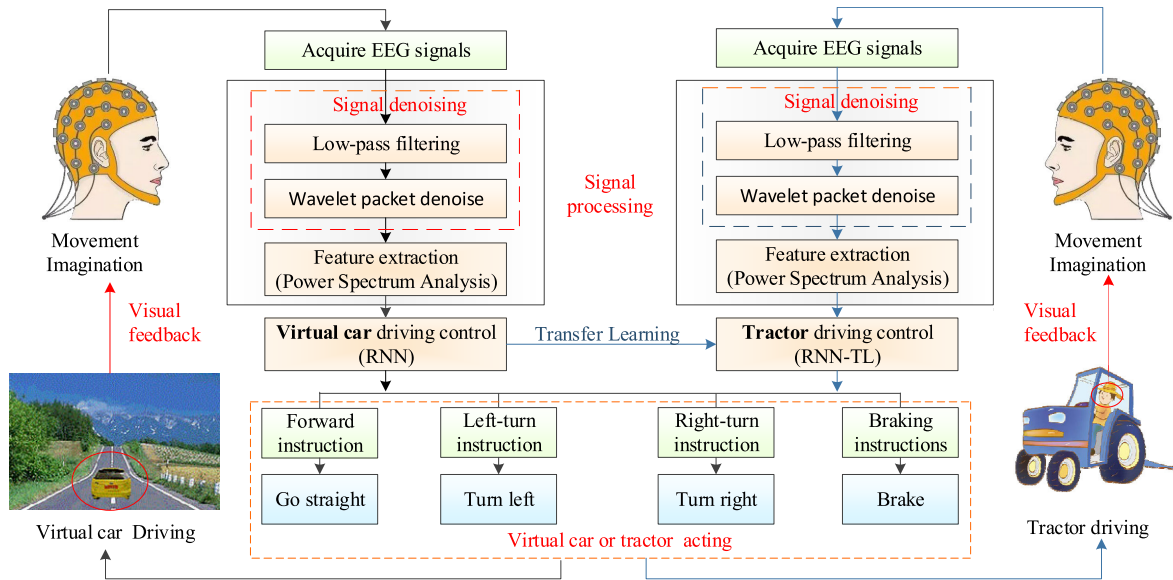


FIGURE 6. The process of EEG control.

were input into the neural network to build the driving model for tractor driving robot control such as straight going, brake, left turn, and right turn.

a: SIGNAL DENOISING

Brainwaves associated with motor imagery are delta (0.5-4 Hz), theta (4-8 Hz), alpha (8-13 Hz), beta (13-30 Hz), and gamma (30-50 Hz) waves which could be captured and processed by Emotiv EPOC+. Also, the frequency of EMG artifact [26] caused by the sub-scalp EMG contraction is generally above 100 Hz. Therefore, the 8th order of 50 Hz Butterworth low-pass filter was used to filter out the high-frequency irrelevant noise signals and the delta, theta, alpha, beta, and gamma waves were extracted.

For denoising the EEG signals, wavelet transform (WT) is a more suitable method to decompose the EEG signal into its different frequency bands and retain the signal information in both time and frequency domain unlike fast Fourier transform (FFT) or short-time Fourier transform (STFT). WT represents or approximates signals or functions through a wavelet function system which is formed by the translation

and stretching of the basic wavelet, then characterized the local characteristics of signals in both time and frequency domains [27]. Besides, the transform coefficients can be approximated to the original signal. Figure 7 shows the detailed denoising method flow.

The continuous WT of signal $x(t)$ is defined as:

$$WT_x(a, \tau) = \frac{1}{\sqrt{a}} \int_{-\infty}^{\infty} x(t)\psi\left(\frac{t-\tau}{a}\right)dt \quad (1)$$

where a represents scale displacement, τ representing time displacement, and $\psi(i)$ is a wavelet basis function, including Haar, db series, Coiflet, and so on.

As EEG signals are discrete signals, discrete wavelet transforms (DWTs) are suitable for discrete wavelets. Compared with the continuous WT, the DWT is to limit the a and τ of the wavelet basis function $\psi(a, \tau)$ to discrete points, that is, the discretization of scale and displacement, and the discrete wavelet basis function is $\psi_{j,k}(t) = 2^{-j/2}\psi(2^{-j}t - k)$, where $j \in Z, k \in Z$, the DWT is:

$$WT_x(j, k) = \int x(t)\psi_{j,k}^*(t)dt \quad (2)$$

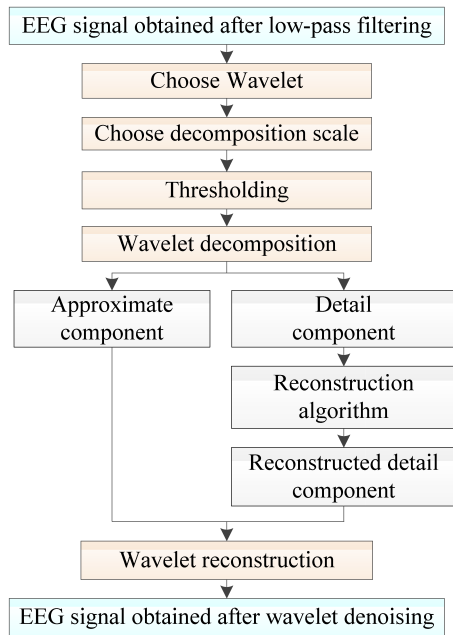


FIGURE 7. The process of noise reduction method based on wavelet transform.

By comparing popular wavelet basis functions, db series has better orthogonality and tight support. So, db wavelet base is selected to better denoising effect. Since brainwaves associated with motor imagery are 5 wavebands, the decomposition scale j is set to 4, and j performs wavelet transformation on the signal $x(t)$ to obtain wavelet decomposition coefficients $WT_x(j, k)$, where k represents the position.

b: FEATURE EXTRACTION BASED ON SPECTRUM

EEG signals are time-varying and nonstationary signals, which have different frequency elements at different times. Besides, the signal amplitude of EEG signal is weak, and it is easily interfered with by the external environment. So, it is hard to analyze EEG signal using FFT. The power spectrum of the random signal could reflect its frequency component and the relative intensity of each component. Therefore, popular power spectrums such as periodograms, MUSIC, and Welch were used to characterize brain commands.

Periodograms method power spectrum treats EEG signals in the time domain as a sequence with limited energy and uses discrete Fourier transform (DFFT) to calculate the power spectral density [28]. The formula for calculating the power spectral density is:

$$P(\omega) = \frac{1}{N} |X_N|^2 = \frac{1}{N} \left| \sum_{n=0}^{N-1} x(n) e^{-j\omega n} \right|^2 \quad (3)$$

where $x(n)$ is the data in the time domain and N is the number of the data.

MUSIC method power spectrum is a non-parametric method of power spectrum estimation based on matrix feature decomposition, which can suppress noise, significantly

improve the signal-to-noise ratio, and can reflect harmonic characteristics in more detail [29]. The basic idea is to separate the signal from the noise, and the spectral estimation calculation formula is shown below:

$$P_{music}(f) = \frac{1}{e^H(f) \left[\sum_{k=p+1}^N V_k V_k^H \right] e(f)} = \frac{1}{\sum_{k=p+1}^N |V_k^H e(f)|^2} \quad (4)$$

where $P_{music}(f)$ is the power spectrum value, f is the complex sine wave frequency, N is the dimension of the eigenvector, V_k is k -order eigenvector of the input signal correlation matrix, p is the dimension of the signal subspace and H is complex conjugate transpose.

Welch method power spectral is a power spectrum density estimator that applies the periodogram, which is based on Bartlett’s idea of splitting the data into segments and finding the average of their periodograms. Where L is the length of the segments, the i -th segment is denoted by x_N^i and the offset of the successive sequences by samples [30]. Compared with the periodic graph, this algorithm performs segmentation through an appropriate window function to make the power spectrum smoother. First, find each segment of the spectrum estimate (5), and then average the L -segment periodic graph to obtain the power spectrum estimate of the entire signal (6).

$$P_x^i \omega = \frac{1}{MU} \left| \sum_{n=0}^{M-1} x_N^i(n) d_2(n) e^{-j\omega n} \right|^2 \quad (5)$$

where $P_x^i \omega$ is the i -th spectral estimate, M is the number of samples in each segment, $U = \frac{1}{M} \sum_{n=0}^{M-1} d_2^2(n)$ is the normalization factor and $d_2(n)$ is added window function.

$$P_{welch}(\omega) = \frac{1}{L} \sum_{i=1}^L P_x^i(\omega) = \frac{1}{MUL} \sum_{i=1}^L \left| \sum_{n=0}^{M-1} x_N^i(n) d_2(n) e^{-j\omega n} \right|^2 \quad (6)$$

where $P_{welch}(\omega)$ is the spectral estimate of the entire signal and L is the number of segments of the periodograms.

c: DRIVING BEHAVIOR RECOGNITION

In the BCI technology, neural networks are more suitable to use for behavior recognition due to their powerful nonlinear fitting and data mining capabilities, such as BP neural networks, Support Vector Machines (SVM), Convolutional Neural Networks (CNN), and Recurrent Neural Networks (RNN), etc. In this article, the above-mentioned neural networks were selected for driving behavior recognition to compare the recognition effects and calculation consumption.

BP is a multi-layer pre-feedback neural network, includes the input layer, hidden layer, and output layer. The learning

process of BP neural network is a forward feedback learning process. It is a process essentially in which errors propagate backward while correcting the weight coefficients of each layer. Feedback learning works through the adjustment of the connection mode, weight, and threshold of each neuron, and the identification of the whole network [31].

The SVM algorithm is based on the statistical learning theory and the Vapnik-Chervonenkis dimension. It maps the input patterns into a higher dimensional feature space through some nonlinear mapping where a linear decision surface is then constructed. In SVM, a kernel function implicitly maps samples to a feature space given by a feature mapping. But, training SVMs from extremely large and complicated datasets is a pivotal issue due to the high time and memory complexity of the SVM training [32], [33]. In this article, RBF was selected as the Kernel function of SVM, the parameters such as c and g were optimized by going through -5 to $+5$ to reach the highest cross-validation accuracy as the best parameters.

In the CNN algorithm, the convolutional layers used are responsible for performing the mathematical process of convolution on the pseudo images generated. Each of these layers is activated by the ReLU, Sigmoid, or Tanh activation functions which determines the output value of each neuron. While the Max pooling Layers are responsible for grouping the original input data, and the dropout layers are responsible for disconnecting a portion of neurons from the previous layer to avoid overfitting in this way. The layers which are between the input layer and the output layer are called hidden layers whose number determines the depth of the architecture. Although it is evident that the greater the depth of the network, the greater the abstraction capacity of the network, however, the greater depth of CNN needs more computational cost to train it [34].

Multilayered architecture is a special architecture of neural models. With respect to the direction of their connection, multilayered networks are divided into feedforward and feedback networks. Highly nonlinear dynamic mappings can be performed by RNNs and therefore have a temporally extended application, whereas multilayer feedforward networks are confined to performing static mappings [35]. So, RNNs are suitable for EEG signals recognition. When processing EEG signals, RNN takes the spectrum of EEG signal as the network input and transmits the output of each layer to the input of the next neural network layer. And at the same time, the output of a hidden layer transmits to its input through a recycled unit to generate its influence, and by this means, each neuron in the hidden layer is recycled, as shown in Figure 8. There is a forward connection and a feedback connection between the neural units of the RNN network. So, the weights are equal, the connection of each neuron is independent and there is no connection with other neurons that contribute to the robustness when processing time series and EEG signals.

While tractor driving utilizing EEG control method in the virtual environment, the subjects drove in every possible

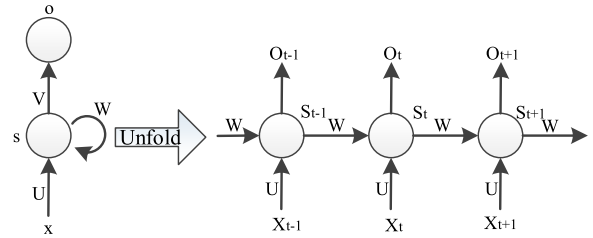


FIGURE 8. RNN hidden layer expansion.

manner they want, including deadly and dangerous way, to generate as complete a training set as possible.

2) TRACTOR DRIVING MODEL BASED ON EEG COMBINED WITH RNN-TL DEEP LEARNING ALGORITHM IN THE ACTUAL ENVIRONMENT

To improve the tractor driving performance through EEG through the tractor driving robot developed by our lab. Transfer Learning (TL) algorithm was applied to transfer the driving experience in the virtual environment to the actual-world only with a small amount of driving experience data in the actual environment.

Training neural networks have faced two critical problems, including expensive resources and computational costs. Besides, the computational time to train a number of deep learning models increases exponentially when the deep neural networks become deeper and more complex. TL is introduced to overcome the problems of expensive resources and computational costs for training multiple deep learning models. TL methodology focuses on applying the gained knowledge of deep learning models from a trained architecture to train another deep learning model on a different task [36].

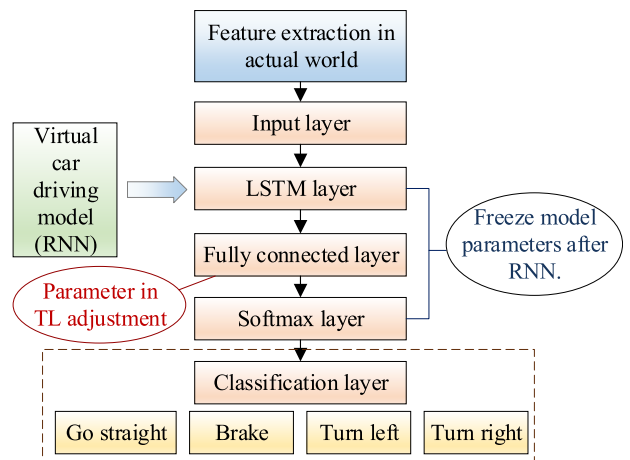


FIGURE 9. Tractor driving model based on RNN-TL.

Specifically, a tractor driving control mode of RNN deep neural network based on EEG was established using the complete dataset built in the virtual environment. Then transfer learning strategy was applied by freezing LSTM layer and Softmax layer followed by training the parameters of a fully connected layer using the small driving data set in the actual field as shown in Figure 9.

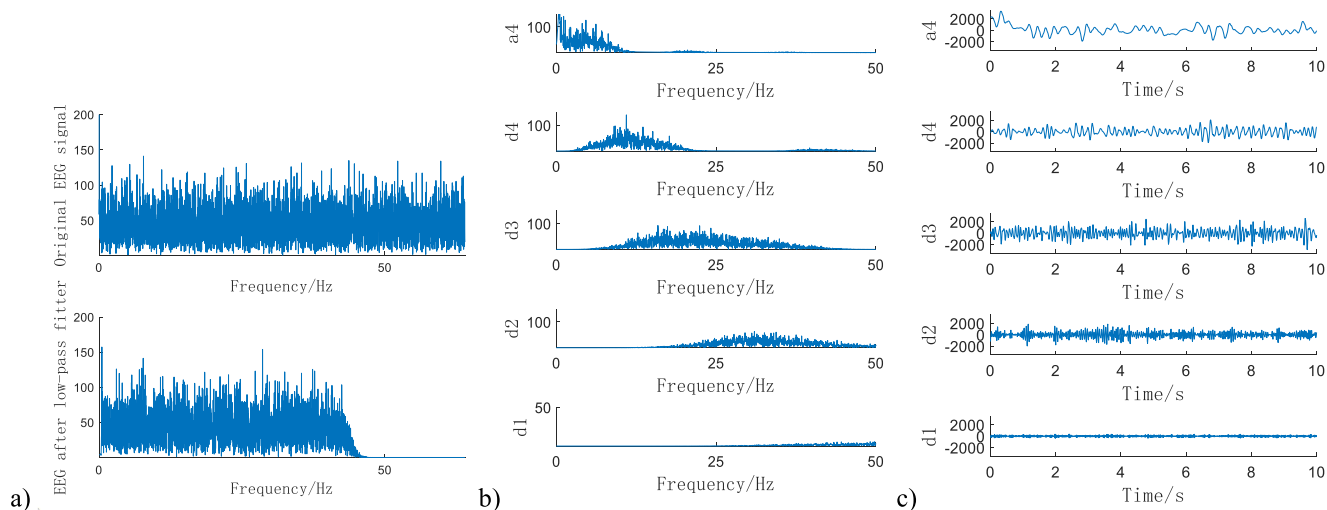


FIGURE 10. Signal denoising (e.g. F3 electrode of left turn signal). a) EEG signal after low-pass filtered. b) Wavelet multi-layer decomposition. c) Wavelet decomposition spectral characteristics.

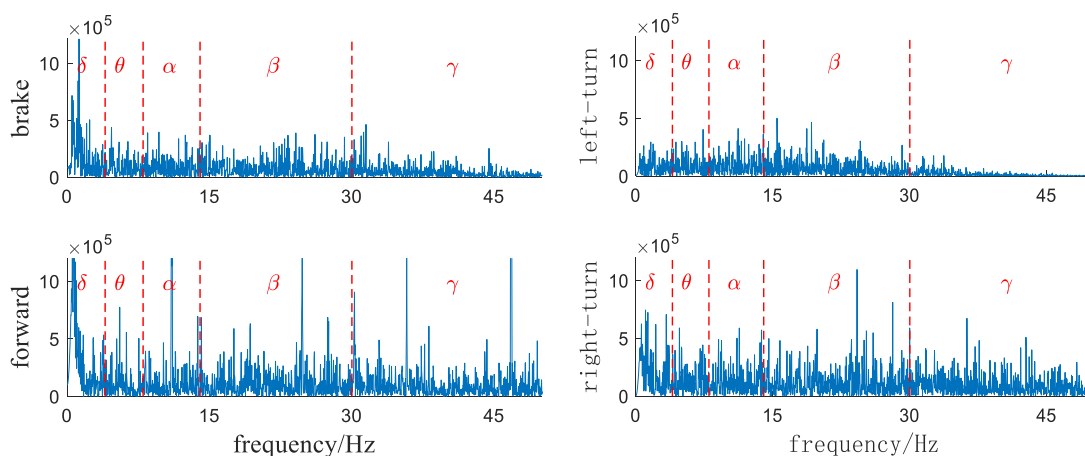


FIGURE 11. Power spectrums of the eeg signals under different control commands.

III. ANALYSIS OF EXPERIMENTAL RESULTS

A. SIGNAL DENOISING

The EEG signals of a driver’s subject are firstly filtered by an 8th order of 50 Hz Butterworth low-pass filter and then decomposed by db4 wavelet packet to remove the high-frequency noise signal d1, as shown in Figure 10.

B. FEATURE EXTRACTION

1) SPECTRIM ANALYSIS

Due to the randomness, time-variability, and vulnerable being interfered with, the power spectrum analysis method was introduced to extract the statistical information of EEG signals for getting the driving control intent with high precision. The power spectrums such as periodograms, MUSIC power spectrum, and Welch power spectrum were selected for comparing the signal-to-noise ratio (SNR) of EEG signal spectrums [37], as shown in Table 1. The Welch power spectrums of EEG signals under different control commands are shown in Figure 11.

TABLE 1. SNR of different power spectrums.

power spectrum	SNR
periodic graph method	2.75×10^{-7}
MUSIC	1.30×10^{-4}
Welch	26.10

As shown in Figure 11, the delta is the frequency range from 0.5 Hz up to 4 Hz, which only occurs in the cortex, and is not controlled by the nerves in the lower parts of the brain. The power spectrum amplitude of this band is significantly larger in the brake and forward control EEG signals. Theta is the frequency range from 4Hz to 8Hz, which can be seen in meditation. The power spectrum amplitude of this band is slightly bigger in the forward and right turn control EEG signals. Alpha is the frequency range from 8Hz to 13Hz, which emerges with relaxation and attenuates with mental exertion. Besides, it can reflect the subconscious mind of the brain. The power spectrum amplitude of this band is

remarkably bigger in the left-turn control EEG signal. The beta is the frequency range from 13 Hz to 30 Hz, which is closely related to consciousness, brain activities, and motor behaviors [38]. The power spectrum amplitude of this band is larger in the forward and right-turn control EEG signals. The gamma is the frequency range from 30 Hz to 50 Hz, which carries out a certain cognitive or motor function. The power spectrum amplitude of this band is bigger in the forward and right-turn control signals. The spectrums of EEG signals of the experimental results are consistent with the law of brain wave activity [39].

TABLE 2. Comprehensive coefficient and weight of electrodes in the right turn signal.

electrodes	AF4	T7	P7	F4	F7	FC6	F3
comprehensive coefficients	0.197	0.092	0.077	0.067	0.063	0.055	0.047
weights	0.263	0.123	0.102	0.089	0.084	0.073	0.063
electrodes	P8	O2	O1	F8	FC5	AF3	T8
comprehensive coefficients	0.047	0.042	0.02	0.016	0.011	0.01	0.006
weights	0.063	0.055	0.027	0.022	0.014	0.013	0.008

2) PCA

Due to the inconvenience to wear and poor experimental comfort using 14 electrodes for EEG signal acquisition, Principle Component Analysis (PCA) algorithm was applied to optimize and reduce the EEG electrodes. The comprehensive coefficient and weight of 14 electrodes e.g. in right turn were obtained in Table 2. And the comprehensive coefficient and weight of each pair of motion control electrodes are shown in Table 3.

TABLE 3. The comprehensive coefficient and weight of each pair of motion control electrodes.

pairs of motion control electrodes	AF3 AF4	F7 F8	T7 T8	F3 F4	O1 O2	P7 P8	FC5 FC6
comprehensive coefficients	0.679	0.619	0.347	0.344	0.335	0.320	0.253
weights	0.234	0.214	0.120	0.119	0.116	0.110	0.087

The results showed that the motion signals such as brake, forward, left-turn, and right-turn mainly reflected on several electrodes which are AF3, AF4, F7, F8, T7, T8, F3, and F4. Besides, the brake control command reflected on the electrodes of AF3, AF4, and F3. The forward control command reflected on the electrodes of AF3, F7, and AF4. The left-turn command reflected on the electrodes of AF3, FC5. The right-turn command reflected on the electrodes of AF4 and T7 respectively. The contribution rate is shown below.

C. DRIVING BEHAVIOR RECOGNITION

Before driving behavior recognition, 1000 groups of EEG driving control signals including brake, forward, left-turn,

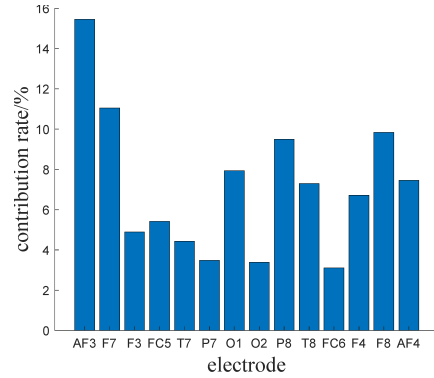


FIGURE 12. The average contribution rate of motion signals in each electrode.

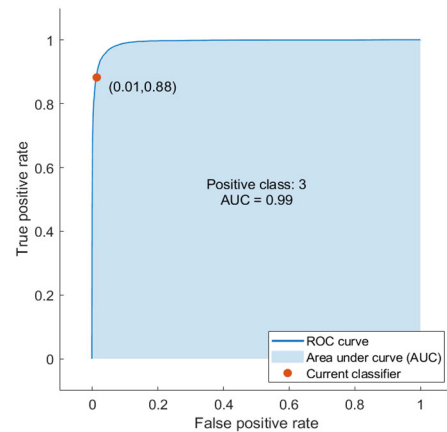


FIGURE 13. The roc curve of RNN-TL algorithm.

and right-turn signals were built in the virtual environment which has 4000 EEG signals. And 750 groups of them were applied as a training set and the rest 250 groups were used as the testing set.

EEG signals of different numbers of the electrode were employed for modeling of driving behavior recognition. The comparing prediction results of the models using BP, SVM, CNN, RNN are shown in Table 4 which demonstrates that more electrodes lead to higher precision at the cost of more time consumption. Moreover, the prediction precision of RNN model is the best among that of different models. Overall, the scheme of 8 electrodes is the optimization in which prediction accuracy and time consumption are 93.1% and 0.48 ms respectively. For the practical application of tractor driving in the actual environment using EEG signal, the transfer learning algorithm was employed. Firstly, 300 groups of EEG driving control signals were built which has 1200 EEG signals. And 200 groups of them were applied as a training set and the rest 100 groups were used as the testing set.

According to the existed RNN model trained using the EEG signals in the virtual environment, the LSTM layer and Softmax layer were frozen firstly followed by training the parameters of the Fully connected layer using the training set of the actual environment to transfer the driving model

TABLE 4. Comparison of different classification methods.

Classification methods	14 electrodes		12 electrodes		10 electrodes		8 electrodes		6 electrodes	
	accuracy /%	test time /ms	accuracy /%	test time /ms	accuracy /%	test time /ms	accuracy /%	test time /ms	accuracy /%	test time /ms
BP	91.3	1.05	89.0	1.02	85.4	0.88	83.1	0.70	74.1	0.59
SVM	91.6	1.25	90.5	1.18	86.9	1.10	81.3	0.95	76.7	0.85
CNN	93.9	0.63	92.9	0.61	91.5	0.57	91.3	0.56	86.1	0.52
RNN	94.5	0.61	92.6	0.57	93.2	0.54	93.1	0.48	89.3	0.42

from virtual environment to the actual environment. Finally, 100 groups of the testing set were used for model testing the result shows that the command recognition accuracy is 93.5% with the time consumption of 0.48 ms. The recall rate is 93.6% and the precision is 93.8%. The ROC curve is shown in Figure 13.

IV. DISCUSSION AND CONCLUSION

A. DISCUSSION

Firstly, the EEG signals of the subjects were collected in the virtual driving environment without any danger to build a complete data set by using the Emotiv-EPOC+ system followed by denoising using 8th order of 50 Hz Butterworth low-pass filter. Then the features of power spectrum signals of driving actions were extracted by the wavelet packet. Furthermore, the obtained features were input into the neural network such as BP, SVM, CNN, and RNN to establish the driving model for tractor driving robot control in a virtual environment such as straight going, brake, left turn, and right turn. Among which the prediction precision of RNN reaches 94.5% followed by CNN with a precision of 93.9%. Whereas the prediction of SVM and BP are only 91.6% and 91.3% respectively. And the calculation time consumption of the RNN model only costs 0.61 ms which leads to an 8.5 mm displacement error when the tractor works at the speed of 50 km/h.

The study of the paper is consistent with the existing research which results show that EEG signal of a human is available to be applied to control machines. For example, the University of Valladolid, Spain [21] studied the control of a tractor tracking specific trajectories based on EEG signals. Silesian Polytechnic University in Poland [18], [19] studied on the basis of EEG aircraft assisted driving to improve the pilot's accident response. Besides, the University of Tokyo in Japan [20] using sEMG to control vehicles to achieve different steering ranges.

To reduce the employed electrodes for improving the user's comfortable feeling, PCA algorithm was applied for dimensionality reduction of electrodes. Eight electrodes were selected which located in the anterior half of the brain, i.e. AF3, AF4, F7, F8, T7, T8, F3, and F4. And the prediction accuracy and time consumptions were 93.1% and 0.48 ms respectively which only lead to 6.7 mm displacement error when the tractor works at the speed of 50 km/h. The motor cortex is mainly located in the central anterior gyrus of the cerebral cortex, where electrodes of AF3 and AF4 are

located in the forehead, electrodes of F3 and F4 are located in the frontal area, and electrodes of F7 and F8 are located in the lateral forehead. Related studies [40] showed that some electrode channels appear more frequently in the subjects, the frontal brain area is more important under artificial induction.

For actual employment in tractor driving control by EEG signals in the actual world, large experimental data should be collected when the subjects drive the tractor using EEG signal. But it's difficult to generate a complete dataset for model training because some driving control will lead to dangerous or even cause death. So, the Transfer Learning algorithm was introduced to use not so many driving experience data in the actual environment to retrain the parameters of the fully connected layer of the trained RNN driving model mentioned above to transfer the EEG signal driving mode from the virtual environment to the actual application world.

Due to the introduction of TL, the improvement of the model accuracy no longer limited to the objective conditions of tractor experiments in the actual environment e.g. site restrictions and natural environment. And the prediction accuracy and time consumptions were 93.5% and 0.48 ms, respectively, with 8 optimized electrodes which lead to only 6.7 mm displacement error when the tractor works at the speed of 50 km/h. The results show that it can meet the conventional requirement of tractor field operations.

In addition, relevant research showed that human movements could be predicted to exceed one second in advance before the movement occurs [41] which means that human-computer cooperative control mode based on EEG could compensate for human reaction delays, improve driving safety, and reduce agricultural machinery accidents caused by improper operation. In the meantime, EEG signal control method can avoid accidents caused by untimely tractor braking and other unexpected conditions for incorrect recognition of control commands or other reasons.

Moreover, the arms and legs of agricultural machinery drivers could be moderately relaxed. Therefore, the work intensity of agricultural machinery drivers could be reduced. Furthermore, this article provides a feasible method for the disabled to drive agricultural machinery.

It should be noted that: during the EEG test, the electrodes of the electroencephalograph need to be kept wet, otherwise the electrodes and the scalp are directly in poor contact, which leads to large errors in the data collected by the electrodes.

B. CONCLUSION

In this article, a tractor assistant driving control method based on EEG signals was proposed to relieve the tight operation to avoid shoulder muscle strain. Also, it can help the driver to avoid misoperation when the brain consciousness and limb movements are not consistent. Furthermore, it can contribute to assist a disabled person to drive tractors as well.

By using deep learning algorithms, there are also many challenges and limitations. For example, a huge dataset is required to obtain better accuracy, but it is difficult to collect huge datasets due to site constraints, environmental influences, and other factors during tractor operation in the actual world. Although it is convenient to build big dataset in the virtual environment, their conditions can not be consistent with each other which require subsequent algorithm modifications.

To solve the incomplete driving data set in the actual world because some driving manners will lead to dangerous or even to death, RNN-TL algorithm was employed by creating the complete driving data in the virtual environment followed by transferring the driving control experience to the actual world with small actual driving data set in the field. The experiments showed the feasibility of the proposed tractor driving control method based on EEG signal combined with RNN-TL deep learning algorithm which can work when the tractor speed is not more than 50 km/h and the displacement error is less than 6.7 mm.

In summary, the paper provided a novel tractor assistant driving control method based on EEG signal and a transferring learning algorithm based on RNN to obtain a perfect control model only using a small dataset in the actual world and large data set in the virtual environment.

REFERENCES

- [1] B. Ma, Y. Yang, Y. Liu, X. Ji, and H. Zheng, "Analysis of vehicle static steering torque based on tire-road contact patch sliding model and variable transmission ratio," *Adv. Mech. Eng.*, vol. 8, pp. 1–11, Sep. 2016.
- [2] S. Zhou, H. Zhao, W. Chen, Z. Miao, Z. Liu, H. Wang, and Y.-H. Liu, "Robust path following of the tractor-trailers system in GPS-denied environments," *IEEE Robot. Autom. Lett.*, vol. 5, no. 2, pp. 500–507, Apr. 2020.
- [3] M. Song, M. S. N. Kabir, S.-O. Chung, Y.-J. Kim, J.-K. Ha, and K.-H. Lee, "Path planning for autonomous lawn mower tractor," *Korean J. Agricult. Sci.*, vol. 42, no. 1, pp. 63–71, Mar. 2015.
- [4] S. Zhang, Y. Wang, Z. Zhu, Z. Li, Y. Du, and E. Mao, "Tractor path tracking control based on binocular vision," *Inf. Process. Agricult.*, vol. 5, no. 4, pp. 422–432, Dec. 2018.
- [5] X. Hu and G. Lodewijks, "Detecting fatigue in car drivers and aircraft pilots by using non-invasive measures: The value of differentiation of sleepiness and mental fatigue," *J. Saf. Res.*, vol. 72, pp. 173–187, Feb. 2020.
- [6] C. Qing, G. Zhong-Ke, Y. Yu-Xuan, D. Wei-Dong, and G. Celso, "Multiple limited penetrable horizontal visibility graph from EEG signals for driver fatigue detection," *Int. J. Neural Syst.*, vol. 29, no. 5, pp. 1–10, 2019.
- [7] R. Sharma, R. B. Pachori, and P. Sircar, "Automated emotion recognition based on higher order statistics and deep learning algorithm," *Biomed. Signal Process. Control*, vol. 58, pp. 1–10, Apr. 2020.
- [8] R. Majid Mehmood, R. Du, and H. J. Lee, "Optimal feature selection and deep learning ensembles method for emotion recognition from human brain EEG sensors," *IEEE Access*, vol. 5, pp. 14797–14806, 2017.
- [9] Z. A. A. Alyasseri, A. T. Khader, M. A. Al-Betar, and O. A. Alomari, "Person identification using EEG channel selection with hybrid flower pollination algorithm," *Pattern Recognit.*, vol. 105, Sep. 2020, Art. no. 107393.
- [10] Z. A. A. Alyasseri, A. T. Khader, M. A. Al-Betar, A. Abasi, S. Makhadmeh, and N. S. Ali, "The effects of EEG feature extraction using multi-wavelet decomposition for mental tasks classification," in *Proc. Int. Conf. Inf. Commun. Technol. (ICICT)*, vol. 19, Apr. 2019, pp. 139–146.
- [11] Z. A. A. Alyasseri, A. T. Khader, M. A. Al-Betar, J. P. Papa, O. A. Alomari, and S. N. Makhadmeh, "Classification of EEG mental tasks using multi-objective flower pollination algorithm for person identification," *Int. J. Integr. Eng.*, vol. 10, no. 7, pp. 102–115, Nov. 2018, doi: 10.30880/ijie.2018.10.07.010.
- [12] Z. A. Alkareem Alyasseri, A. T. Khader, M. A. Al-Betar, J. P. Papa, O. A. Alomari, and S. N. Makhadmeh, "An efficient optimization technique of EEG decomposition for user authentication system," in *Proc. 2nd Int. Conf. BioSignal Anal., Process. Syst. (ICBAPS)*, Jul. 2018, pp. 1–6.
- [13] Z. A. A. Alyasseri, A. T. Khader, M. A. Al-Betar, J. P. Papa, and O. A. Alomari, "EEG-based person authentication using multi-objective flower pollination algorithm," in *Proc. IEEE Congr. Evol. Comput. (CEC)*, Jul. 2018, pp. 1–8.
- [14] Z. A. A. Alyasseri, A. T. Khader, M. A. Al-Betar, A. K. Abasi, and S. N. Makhadmeh, "EEG signals denoising using optimal wavelet transform hybridized with efficient metaheuristic methods," *IEEE Access*, vol. 8, pp. 10584–10605, 2020.
- [15] Z. A. A. Alyasseri, A. T. Khader, M. A. Al-Betar, J. P. Papa, and O. A. Alomari, "EEG feature extraction for person identification using wavelet decomposition and multi-objective flower pollination algorithm," *IEEE Access*, vol. 6, pp. 76007–76024, 2018.
- [16] L. Minati, N. Yoshimura, and Y. Koike, "Hybrid control of a vision-guided robot arm by EOG, EMG, EEG biosignals and head movement acquired via a consumer-grade wearable device," *IEEE Access*, vol. 4, pp. 9528–9541, 2016.
- [17] V. Gandhi, G. Prasad, D. Coyle, L. Behera, and T. M. McGinnity, "EEG-based mobile robot control through an adaptive Brain-Robot interface," *IEEE Trans. Syst., Man, Cybern., Syst.*, vol. 44, no. 9, pp. 1278–1285, Sep. 2014.
- [18] B. Biniyas, D. Myszor, H. Palus, and K. A. Cyran, "Prediction of pilot's reaction time based on EEG signals," *Frontiers Neuroinform.*, vol. 14, pp. 1–13, Feb. 2020.
- [19] B. Biniyas, D. Myszor, and K. A. Cyran, "A machine learning approach to the detection of Pilot's reaction to unexpected events based on EEG signals," *Comput. Intell. Neurosci.*, vol. 2018, pp. 1–9, Oct. 2018.
- [20] E. J. C. Nacpil, R. Zheng, T. Kaizuka, and K. Nakano, "A surface electromyography controlled steering assistance interface," *J. Intell. Connected Vehicles*, vol. 2, no. 1, pp. 1–13, Aug. 2019.
- [21] J. Gomez-Gil, I. San-Jose-Gonzalez, L. F. Nicolas-Alonso, and S. Alonso-Garcia, "Steering a tractor by means of an EMG-based human-machine interface," *Sensors*, vol. 11, no. 7, pp. 7110–7126, Jul. 2011.
- [22] W. Lu, H. Chen, L. Wang, X. Zhao, and Y. Zhang, "Motion analysis of tractor robot driver's gear shift mechanical arm," *Trans. Chin. Soc. Agricult. Mach.*, vol. 47, no. 1, pp. 37–44, 2016.
- [23] H. Chen, W. Lu, and X. L. Zhao, "The fuzzy-adaptive PID control based on the force feedback of the tractor robot driver's gear shift mechanical arm," *J. Nanjing Agricult. Univ.*, vol. 39, no. 1, pp. 166–174, 2016.
- [24] W. Lu, H. Chen, J. Wang, L. Wang, W. Qiu, and Y. Deng, "Research on human-computer cooperation method based on tractor driving robot," *J. Nanjing Univ. Inf. Sci. Technol., Natural Sci. Ed.*, vol. 11, no. 2, pp. 165–172, 2019.
- [25] N. Cudlenco, N. Popescu, and M. Leordeanu, "Reading into the mind's eye: Boosting automatic visual recognition with EEG signals," *Neurocomputing*, vol. 386, pp. 281–292, Apr. 2020.
- [26] S. Ren, S. V. Gliske, D. Brang, and W. C. Stacey, "Redaction of false high frequency oscillations due to muscle artifact improves specificity to epileptic tissue," *Clin. Neurophysiol.*, vol. 130, no. 6, pp. 976–985, Jun. 2019.
- [27] M. K. Wali, M. Murugappan, and B. Ahmmad, "Wavelet packet transform based driver distraction level classification using EEG," *Math. Problems Eng.*, vol. 2013, Nov. 2013, Art. no. 297587.
- [28] J. T. VanderPlas, "Understanding the Lomb-Scargle periodogram," *Astrophys. J. Suppl. Ser.*, vol. 236, no. 1, p. 16, May 2018.
- [29] X. Sun and L. Sun, "Harmonic frequency estimation based on modified-music algorithm in power system," *Open Electr. Electron. Eng. J.*, vol. 9, no. 1, pp. 28–42, 2015.

- [30] Z. Zhao, L. Yang, D. Chen, and Y. Luo, "A human ECG identification system based on ensemble empirical mode decomposition," *Sensors*, vol. 13, no. 5, pp. 6832–6864, May 2013.
- [31] L. Liu, "Recognition and analysis of motor imagery EEG signal based on improved bp neural network," *IEEE Access*, vol. 7, pp. 47794–47803, 2019.
- [32] X. Li, X. Chen, Y. Yan, W. Wei, and Z. Wang, "Classification of EEG signals using a multiple kernel learning support vector machine," *Sensors*, vol. 14, no. 7, pp. 12784–12802, Jul. 2014.
- [33] J. Nalepa and M. Kawulok, "Selecting training sets for support vector machines: A review," *Artif. Intell. Rev.*, vol. 52, no. 2, pp. 857–900, Aug. 2019.
- [34] Q. Liu, J. Cai, S.-Z. Fan, M. F. Abbod, J.-S. Shieh, Y. Kung, and L. Lin, "Spectrum analysis of EEG signals using CNN to model Patient's consciousness level based on anesthesiologists' experience," *IEEE Access*, vol. 7, pp. 53731–53742, 2019.
- [35] S. Z. Rose Yu, A. Anandkumar, and Y. Yue, "Long-term forecasting using higher-order tensor RNNs," *J. Mach. Learn. Res.*, vol. 1, pp. 1–24, Oct. 2019.
- [36] T. Le, M. T. Vo, T. Kieu, E. Hwang, S. Rho, and S. W. Baik, "Multiple electric energy consumption forecasting using a cluster-based strategy for transfer learning in smart building," *Sensors*, vol. 20, no. 9, p. 2668, May 2020.
- [37] A. Suarez-Perez, G. Gabriel, B. Rebollo, X. Illa, A. Guimerà-Brunet, J. Hernández-Ferrer, M. T. Martínez, R. Villa, and M. V. Sanchez-Vives, "Quantification of signal-to-noise ratio in cerebral cortex recordings using flexible MEAs with co-localized platinum black, carbon nanotubes, and gold electrodes," *Frontiers Neurosci.*, vol. 12, p. 862, Nov. 2018.
- [38] M. Roohi-Azizi, L. Azimi, S. Heysieattalab, and M. Aamidfar, "Changes of the brain's bioelectrical activity in cognition, consciousness, and some mental disorders," *Med. J. Islamic Republic Iran*, vol. 31, p. 53, Sep. 2017.
- [39] R. M. Mehmood and H. J. Lee, "Exploration of prominent frequency wave in EEG signals from brain sensors network," *Int. J. Distrib. Sensor Netw.*, vol. 11, no. 11, Nov. 2015, Art. no. 386057.
- [40] N. Masood and H. Farooq, "Investigating EEG patterns for dual-stimuli induced human fear emotional state," *Sensors*, vol. 19, pp. 1–22, Jan. 2019.
- [41] O. Bai, V. Rathi, P. Lin, D. Huang, H. Battapady, D.-Y. Fei, L. Schneider, E. Houdayer, X. Chen, and M. Hallett, "Prediction of human voluntary movement before it occurs," *Clin. Neurophysiol.*, vol. 122, no. 2, pp. 364–372, Feb. 2011.



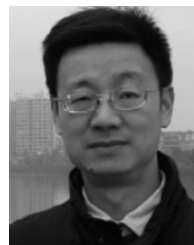
JINXIA YUAN received the master's and Ph.D. degrees in education science from Nanjing Normal University, China, in 2005 and 2008, respectively. She has been an Associate Professor since 2012. Her research interests include preschool curriculum and educational evaluation using advanced technology.



YIMING DENG (Senior Member, IEEE) received the B.S. degree in electrical engineering from Tsinghua University, Beijing, China, in 2003, and the Ph.D. degree in electrical engineering from Michigan State University, East Lansing, MI, USA, in 2009. He is currently an Associate Professor with the Nondestructive Evaluation Laboratory, Electrical and Computer Engineering Department, College of Engineering, Michigan State University. His current research interests include electromagnetic and acoustic nondestructive evaluation structural health monitoring for multiscale, multiresolution, and multiparameter damage diagnostics and prognostics, applied electromagnetics, acoustics, and computational modeling. He is a member of ASNT. He serves as a Reviewer for the U.S. Department of Transportation and the NDSEG Program (U.S. DoD and ASEE). He is an Associate Editor of the *IEEE TRANSACTIONS ON RELIABILITY*, *Materials Evaluation*, the *International Journal of Prognostics and Health Management*, and *RAMS Proceedings*.

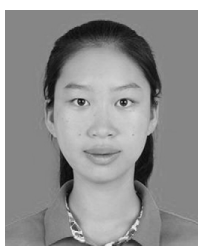


WEI LU (Member, IEEE) received the master's degree in measurement technology and instrument and the Ph.D. degree in instrument science and technology from Southeast University, China, in 2005 and 2012, respectively. He was an Assistant Professor with Nanjing Agricultural University, from 2012 to 2014, where he has been an Associate Professor, since 2015. He was also a Visiting Scholar with Michigan State University, from 2016 to 2018. His current research interests include intelligent robotics and advanced non-destructive detection technology in agriculture. He became a member of ASABE in 2017; and the Director of the Jiangsu Province Instrument and Control Society in China, in 2015, and the Jiangsu Province Automatics Society in China, in 2016.



AIGUO SONG (Senior Member, IEEE) was born in Huangshan, China, in 1968. He received the B.S. degree in automatic control and the M.S. degree in measurement and control from the Nanjing University of Aeronautics and Astronautics, Nanjing, China, in 1990 and 1993, respectively, and the Ph.D. degree in measurement and control from Southeast University, Nanjing, in 1996.

From 1996 to 1998, he was an Associate Researcher with the Intelligent Information Processing Laboratory, Southeast University. From 1998 to 2000, he was an Associate Professor with the Department of Instrument Science and Engineering, Southeast University. From 2000 to 2003, he was the Director of the Robot Sensor and Control Laboratory, Southeast University. From 2003 to 2004, he was a Visiting Scientist with the Laboratory for Intelligent Mechanical Systems, Northwestern University, Evanston, IL, USA. He is currently a Professor with the School of Instrument Science and Engineering, Southeast University. His current research interests include teleoperation, haptic display, the Internet Telerobotics, and distributed measurement systems.



YUNING WEI is currently pursuing the bachelor's degree with Nanjing Agricultural University, Nanjing, China. Her current research interest includes robotic technology.

...